SUPPLEMENTARY MATERIALS

Supplementary Fig. 1 to 14

Supplementary Table 1 to 4

SUPPLEMENTARY FIGURE AND TABLE LEGENDS

Supplementary Fig. 1. Characterization of the doxycycline inducible THP-1 cell lines. (a) Schematic diagram of the lentiviral vector (pTRIPZ) used to construct the inducible cell lines. Abbreviations: TRE, Tet-responsive element; T2A, 2A sequence from *Thosea asigna*; GFP, green fluorescent protein; UBC, Ubiquitin C promoter; rtTA3, reverse tetracycline-transactivator 3; IRES, internal ribosomal entry site; $Puro^R$, puromycin resistance gene. **(b)** Histograms showing GFP fluorescence of the inducible cell lines in the absence and presence of doxycycline (2 ug/mL) after 3 days of induction. The data shown is representative of 4 independent experiments. **(c)** Western blot for the 2A peptide tagged to the C-terminus of IDH1 in lysates generated from the inducible cell lines without or with doxycycline induction for 4 days. β-actin levels were probed as loading controls. The data shown is representative of 2 independent experiments. **(d)** Intracellular flow cytometry staining for mutant IDH1 R132H expression in the inducible cell lines after 3 days of induction. The data shown is representative of 3 independent experiments. **(e)** Measurement of intracellular 2-HG levels in the inducible cell lines after 7 days of induction with doxycycline. The signal intensity of 2-HG was normalized to the glutamate peak for each sample. The data shown represents the fold-increase in normalized 2-HG levels relative to the uninduced sample.

Supplementary Fig. 2. Measurement of the degree of BCL-2 knockdown by lentiviral shRNA vectors using intracellular flow cytometry. Intracellular flow cytometry staining for BCL-2 expression in THP-1 cells 8 days following transduction with the indicated shRNA lentiviral vectors. The red histograms represent non-specific staining with an isotype control antibody (mouse IgG1, kappa) conjugated to BD Horizon V450. The blue histograms represent

specific BCL-2 staining. The degree of knockdown (k/d) is shown on the top right of each panel. The data shown is representative of two independent experiments.

Supplementary Fig. 3. Mutant IDH2 expression and octyl-(R)-2-HG treatment increase sensitivity to ABT-199 in AML cell lines and cord blood CD34$^+$ HSPCs. (a) Parental THP-1 cells were transduced with lentiviral vectors that constitutively expressed WT IDH2, mutant IDH2 R140Q, or mutant IDH2 R172K. Four days after transduction, transduced (GFP$^+$) cells were FACS-purified and treated with serial dilutions of ABT-199 at the indicated concentrations. Cell viability was determined by Annexin V staining 3 days after treatment and was normalized to the untreated control sample. The data shown are the means of three biological replicates with errors bars showing standard deviation. **(b)** Seven AML cell lines were treated with serial dilutions of ABT-199 at the indicated concentrations in the absence or presence of octyl-(R)-2-HG (650μM for KG-1, 750μM for TF-1, 700μM for OCI-AML3, 650μM for HEL, 400μM for U937, 550μM for NB4, and 400μM for Kasumi-1). Cell viability was determined by Annexin V staining 1-2 days after ABT-199 treatment and was normalized to the untreated control sample. The data shown are the means of three biological replicates with errors bars showing standard deviation. **(c)** CD34$^+$ enriched cord blood HSPCs were exposed to octyl-(R)-2-HG at 600μM or PBS (untreated control) and ABT-199 at 500nM. Cell viability was determined by Annexin V staining 2 days after ABT-199 treatment. Data shown is representative of three independent biological replicates. **(d)** Treatment with octyl-(R)-2-HG fails to sensitize AML cells to doxorubicin and cytarabine. THP-1 or KG-1 cells were exposed to octyl-(R)-2-HG at the indicated concentrations or PBS (untreated control) and serial dilutions of doxorubicin or cytarabine at the indicated concentrations. Cell viability was determined by Annexin V staining 2

or 3 days after treatment with the cytotoxic agents. The data shown is from one set of experiments.

Supplementary Fig. 4. FACS-sorting strategy for the viable blast population in primary human AML samples. See Online Methods for details.

Supplementary Fig. 5. Effect of ABT-199 treatment on hematologic parameters and weight of human AML engrafted NSG mice. Weight and complete blood counts (CBC) were determined before and after 7 days of treatment with ABT-199. The data shown represent the percentage change relative to pre-treatment baseline values. Each data point represents an individual animal. The horizontal line represents the mean of each group with error bars indicating standard deviation. Abbreviations: N.S. non-significant.

Supplementary Fig. 6. Improved survival of primary recipients treated with ABT-199 and secondary recipients transplanted with bone marrow cells collected from ABT-199 treated primary recipients. (a) Kaplan-Meier survival curves of primary NSG recipients engrafted with the indicated samples following mock or ABT-199 treatment. The treatment period is as indicated on each graph. n=4 for each treatment group. **(b)** Kaplan-Meier survival curves of secondary transplant recipients of bone marrow cells from vehicle or ABT-199-treated NSG mice engrafted with the indicated samples. n=5 for each treatment group.

Supplementary Fig. 7. (a) Increase in BCL-2 dependence is not correlated with changes in expression of BCL-2 family members. Left panel: Parental THP-1 cells were treated with

octyl-(R)-2-HG (300μM) for 48 hours. Whole cell lysates were prepared from the treated cells and probed for expression of the indicated proteins by Western blot. β-actin levels were probed as loading controls. The data shown is representative of two independent experiments. **Right panel:** The indicated inducible THP-1 cell lines were treated with doxycycline at 2μg/mL for 4 days. Whole cell lysates prepared from the induced cells and untreated control cells were probed for expression of the indicated proteins by Western blot. β-actin levels were probed as loading controls. Western blot for the 2A peptide tagged to the C-terminus of IDH1 in lysates was performed to confirm cDNA expression. The data shown is representative of two independent experiments. **(b) Treatment with antioxidants fails to rescue the synthetic lethal phenotype.** Parental THP-1 cells were exposed to the indicated antioxidants and treated with DMSO or ABT-199 (200nM) in the absence or presence of octyl-(R)-2-HG at 300μM. Viability was determined by annexin V staining 24 hours after treatment. The concentrations used for each antioxidant were as follows: ebselen, 20uM; glutathione monoethyl ester, 10mM; MnTBAP, 100uM; MnTMPyP, 100uM; NAC (N-acetylcystinine), 10mM; PEG-CAT (PEGylated-catalase) 500U/mL; PEG-SOD (PEGylated-superoxide dismutase) 100U/mL; TEMPOL, 1mM; Tiron, 1mM; and Trolox, 200μM.

Supplementary Fig. 8. (a) (S)-2-HG fails to accelerate the collapse of $\Delta\Psi_{mito}$ upon ABT-199 treatment. Intact functional mitochondria were isolated from THP-1 cells and incubated with the indicated treatments and JC-1. Kinetic changes in JC-1 fluorescence were measured and reported as JC-1 fluorescence values normalized to the maximum for each condition. The data shown are representative of three independent experiments. **(b) (R)-2-HG does not inhibit complex V activity.** Enzymatic activity of complex V of the electron transport chain (ETC) was

determined in the presence of (R)-2-HG at 10mM. The data shown are the means of three biological replicates with error bars showing standard deviation. Abbreviations: n.s., not significant.

Supplementary Fig. 9. The (R)-enantiomer of 2-HG alters the absorbance spectrum of reduced COX and the changes are reversible with cyanide treatment. (a) The absorbance spectrum in the Soret region (390nm to 490nm) of oxidized or reduced COX was measured after the addition of either (R)-2-HG, (S)-2-HG, or cyanide at the indication concentrations for 1 hour at room temperature. **(b)** Cyanide (10mM) or water (negative control) was added to a solution of reduced COX pre-incubated with (R)-2-HG. After a 1-hour incubation at room temperature, the absorbance spectrum was again measured. The data shown are representative of two independent experiments.

Supplementary Fig. 10. COX activity is suppressed in THP-1 cells exposed to octyl-(R)-2-HG. (a) THP-1 cells were pre-treated with octyl-(R)-2-HG at 350μM for 3 days or PBS as untreated control. The oxygen consumption rates (OCR) of the cells were then serially measured using the Seahorse extracellular flux analyzer at baseline and following injection of carbonyl cyanide-*4*-(trifluoromethoxy)phenylhydrazone (FCCP), antimycin A (AA), *N,N,N′,N′*-tetramethyl-*p*-phenylenediamine/sodium ascorbate (TMPD/A), and sodium azide (NaN_3) into the analysis well. Error bars represent standard deviations derived from technical replicates. Data shown is representative of two independent experiments. **(b)** THP-1 cells treated as described in (a) were stained with MitoTracker Green FM to quantify the mitochondrial mass in each condition. Data shown is representative of two independent experiments.

Supplementary Fig. 11. Chemical inhibition of COX activity sensitizes AML cell lines to ABT-199. KG-1 and Kasumi-1 cells were untreated or treated with sodium azide (2.5mM) or potassium cyanide (5mM) and serial dilutions of ABT-199 at the indicated concentrations. Cell viability was determined 48 hours after treatment by Annexin V staining. The data shown are the means of three biological replicates with error bars showing standard deviation.

Supplementary Fig. 12. Knockdown of COX-IV expression reduces COX enzymatic activity. (a) THP-1 and KG-1 cells were transduced with a non-targeting control (Ctrl) or COX-IV shRNA lentiviral vector. Whole cell lysates from FACS-sorted transduced (RFP^+) cells were probed for COX-IV levels by immunoblotting with β-actin as loading control. The data shown is representative of two independent experiments. **(b)** The oxygen consumption rates (OCR) of the FACS-sorted transduced (RFP^+) cells were serially measured using the Seahorse extracellular flux analyzer at baseline and following injection of (FCCP), antimycin A (AA), *N,N,N′,N′*-tetramethyl-*p*-phenylenediamine/sodium ascorbate (TMPD/A), and sodium azide (NaN_3) into the analysis well. Error bars represent standard deviations derived from technical replicates. Data shown is representative of three independent experiments.

Supplementary Fig. 13. Tigecycline treatment reduces MT-CO1 levels and COX enzymatic activity. (a) THP-1, KG-1, and Kasumi-1 cells were treated with DMSO (vehicle control) or tigecycline at 10uM (THP-1, KG-1) or 2.5uM (Kasumi-1) for 48 hours and stained for intracellular MT-CO1 expression using an Alexa Fluor 488-conjugated antibody. The data shown is representative of two independent experiments. **(b)** The oxygen consumption rates

(OCR) of the cells treated as described in (a) were serially measured using the Seahorse extracellular flux analyzer at baseline and following injection of (FCCP), antimycin A (AA), *N,N,N′,N′*-tetramethyl-*p*-phenylenediamine/sodium ascorbate (TMPD/A), and sodium azide (NaN_3) into the analysis well. Error bars represent standard deviations derived from technical replicates. Data shown is representative of three independent experiments.

Supplementary Fig. 14. Proposed model of synthetic lethal mechanism between (R)-2-HG and BCL-2 inhibition. Left panel: Electrons from NADH and succinate are transferred through the ETC to oxygen which is reduced to water. In the process, protons are pumped from the matrix into the intermembrane space generating the $\Delta\Psi_{mito}$. Middle panel: (R)-2-HG-mediated inhibition of cytochrome C oxidase (COX; complex IV) activity generates an activating signal to BAX/BAK, but their activation is blocked by BCL-2, thereby maintaining cell viability. Right panel: Simultaneous inhibition of COX by (R)-2HG and BCL-2 activity by ABT-199 permits the full activation and oligomerization of BAX/BAK resulting in MOMP, and commitment to apoptosis.

Supplementary Table 1. List of synthetic lethal gene hits from the screen.

Supplementary Table 2. Clinical characteristics, cytogenetics, mutation status of FLT3, NPM1, and IDH1/2, and ABT-199 IC_{50} of primary AML samples. De novo AML samples were collected at the time of diagnosis. Primary refractory samples were collected after induction chemotherapy that failed to achieve a complete remission (CR). Relapsed samples were collected at the time of relapse following a morphologic CR. Progression samples were collected at the

time of progression following a partial remission with a lower-intensity regimen (e.g. hypomethylating agents). Abbreviations: MDS, myelodysplastic syndrome; CMML, chronic myelomonocytic leukemia; FAB, French American British; WHO, World Health Organization; PV, polycythemia vera; ITD, internal tandem duplication; TKD, tyrosine kinase domain.

Supplementary Table 3. Bone marrow engraftment levels of NSG mice transplanted with primary human AML samples before and after treatment with vehicle (mock) or ABT-199 for 7 consecutive days. * SU430 is a mixed phenotype acute leukemia sample (B/myeloid) with variable CD33 and CD19 expression on blasts. Leukemic engraftment of SU430 was determined based on human CD45 expression alone.

Supplementary Table 4. List of primary AML samples, IDH genotype, MT-CO1 expression level, unnormalized and normalized COX activity.

Supplementary Figure 1

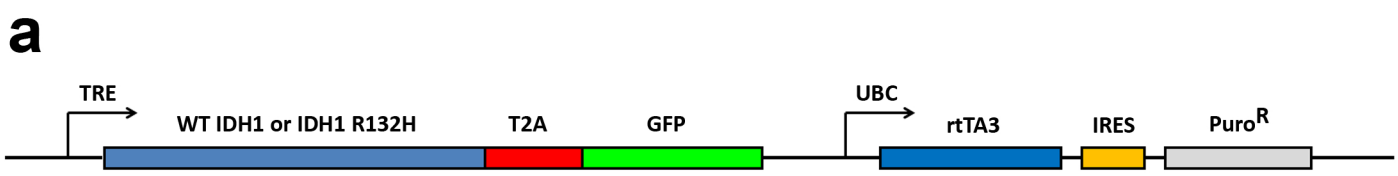

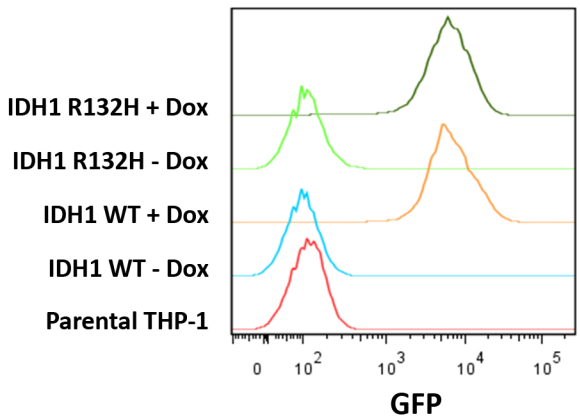

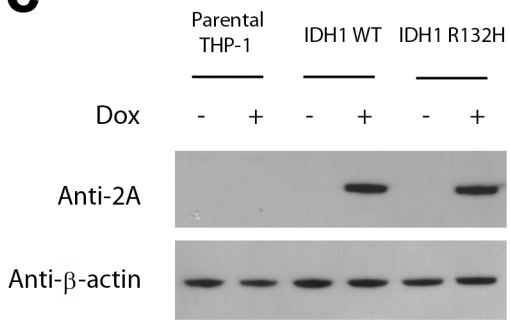

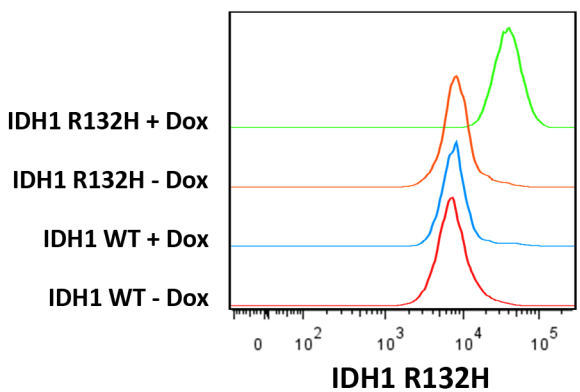

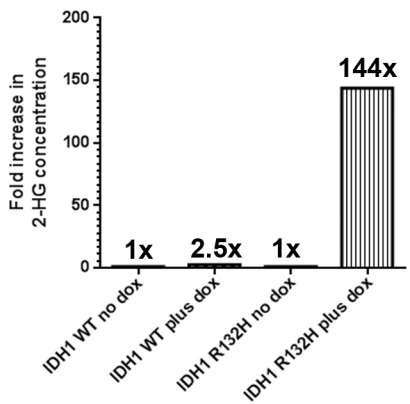

Supplementary Figure 2

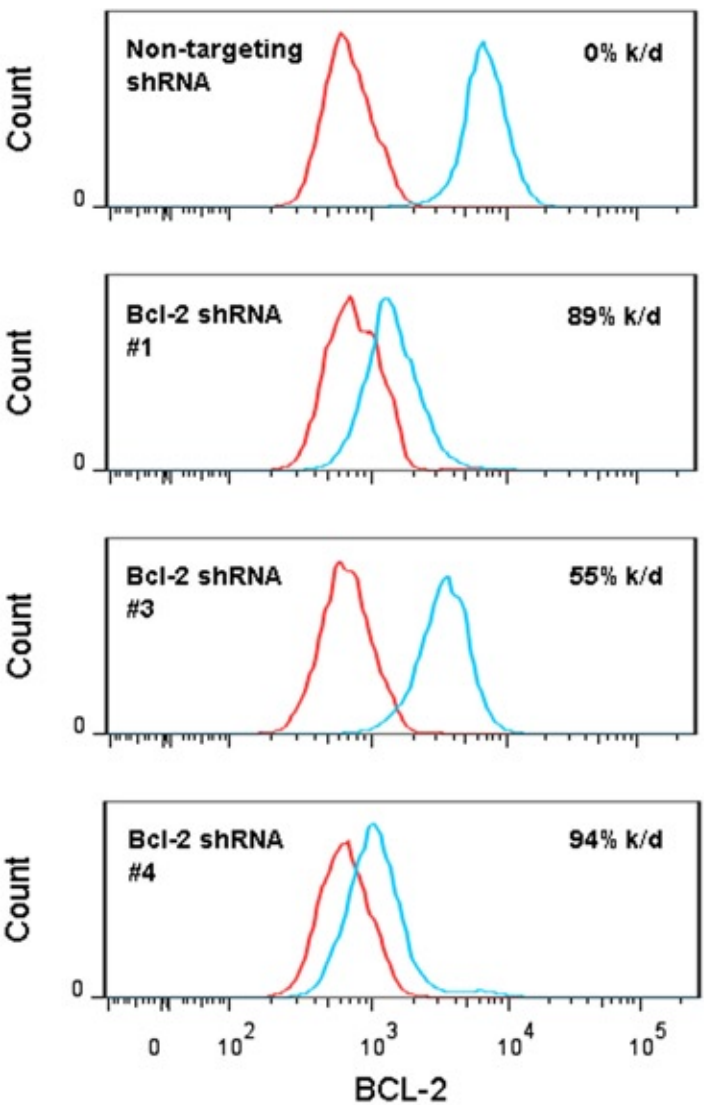

Supplementary Figure 3

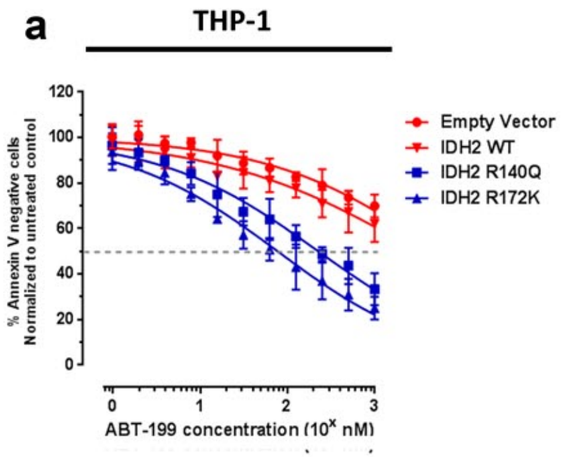

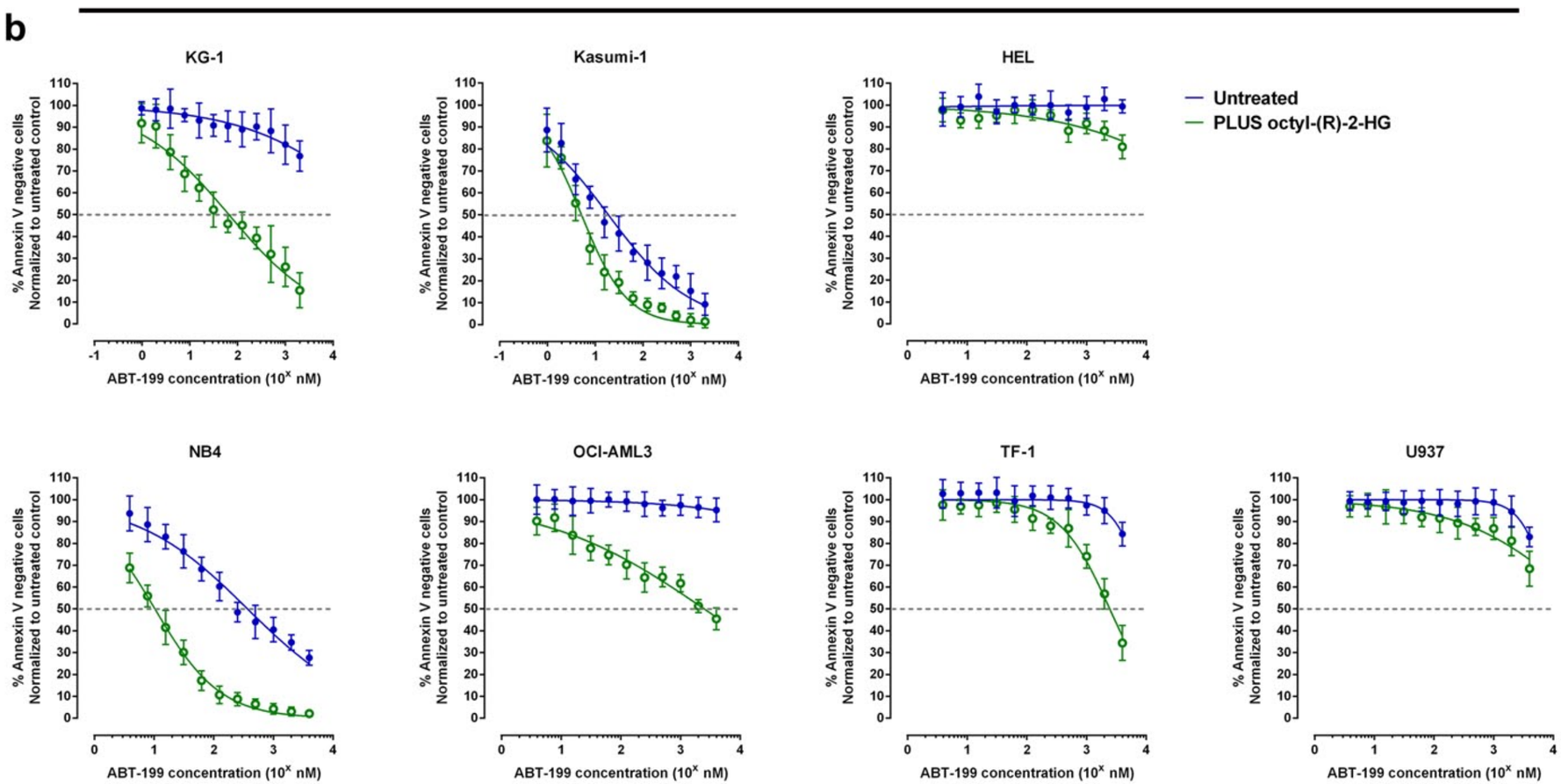

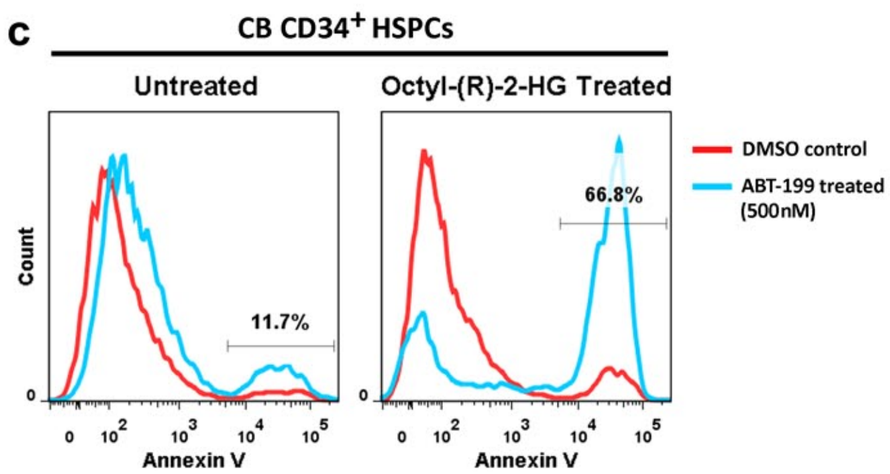

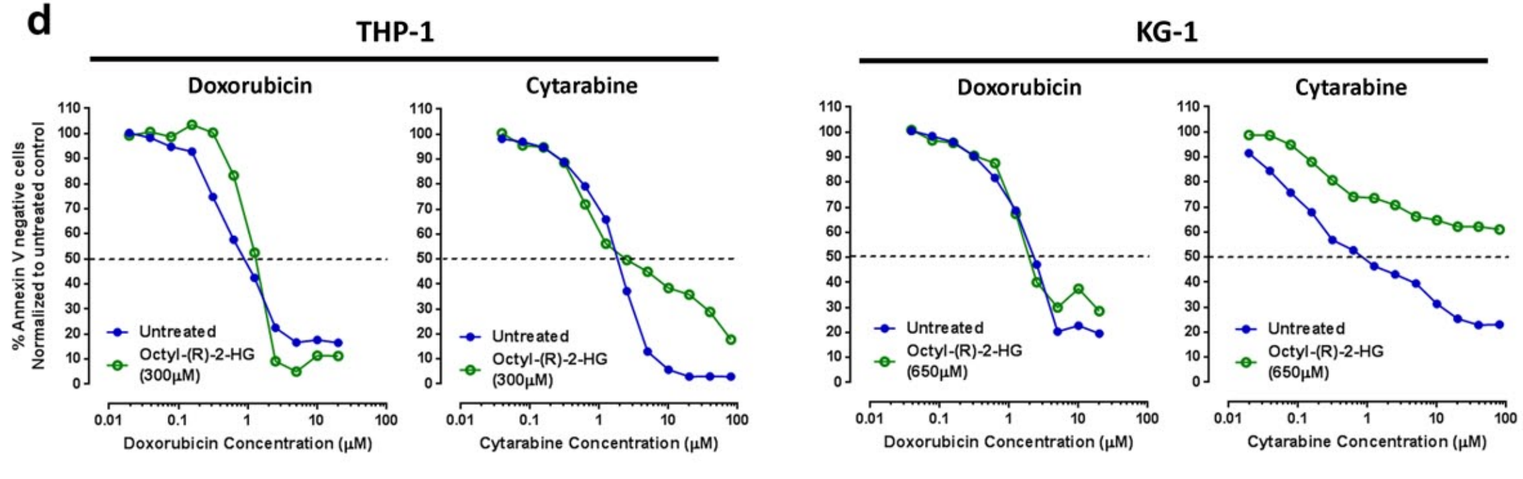

Supplementary Figure 4

Pre-sort

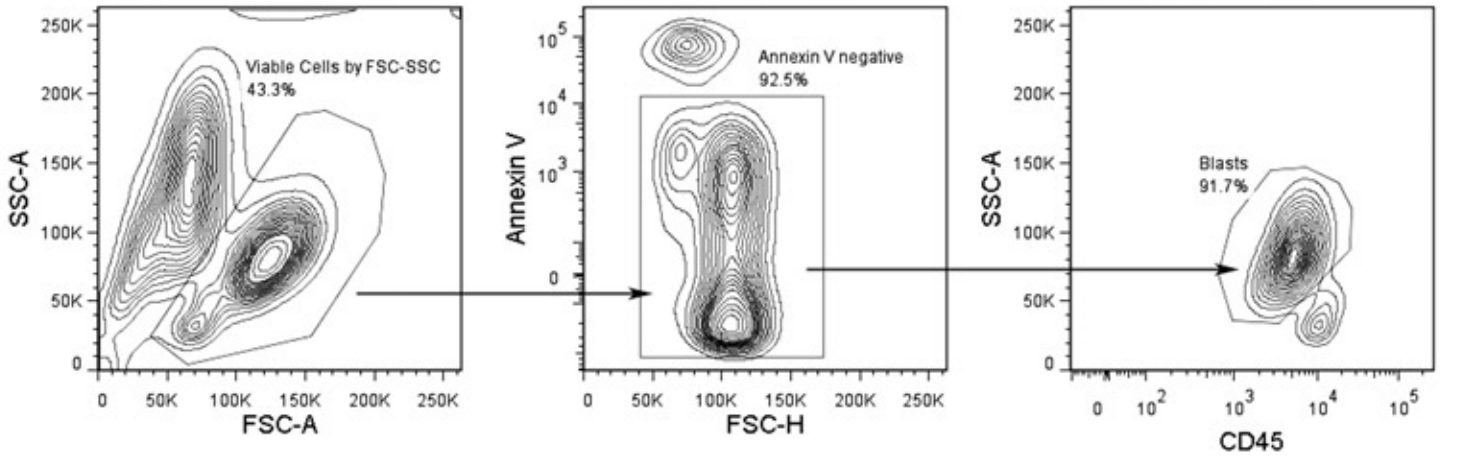

Post-sort

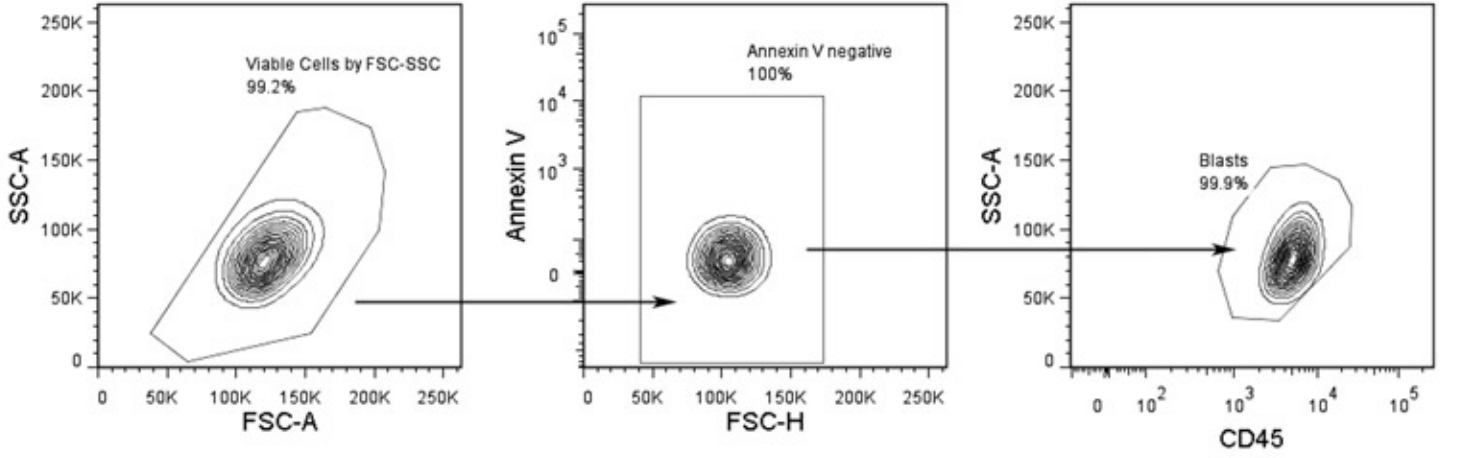

Supplementary Figure 5

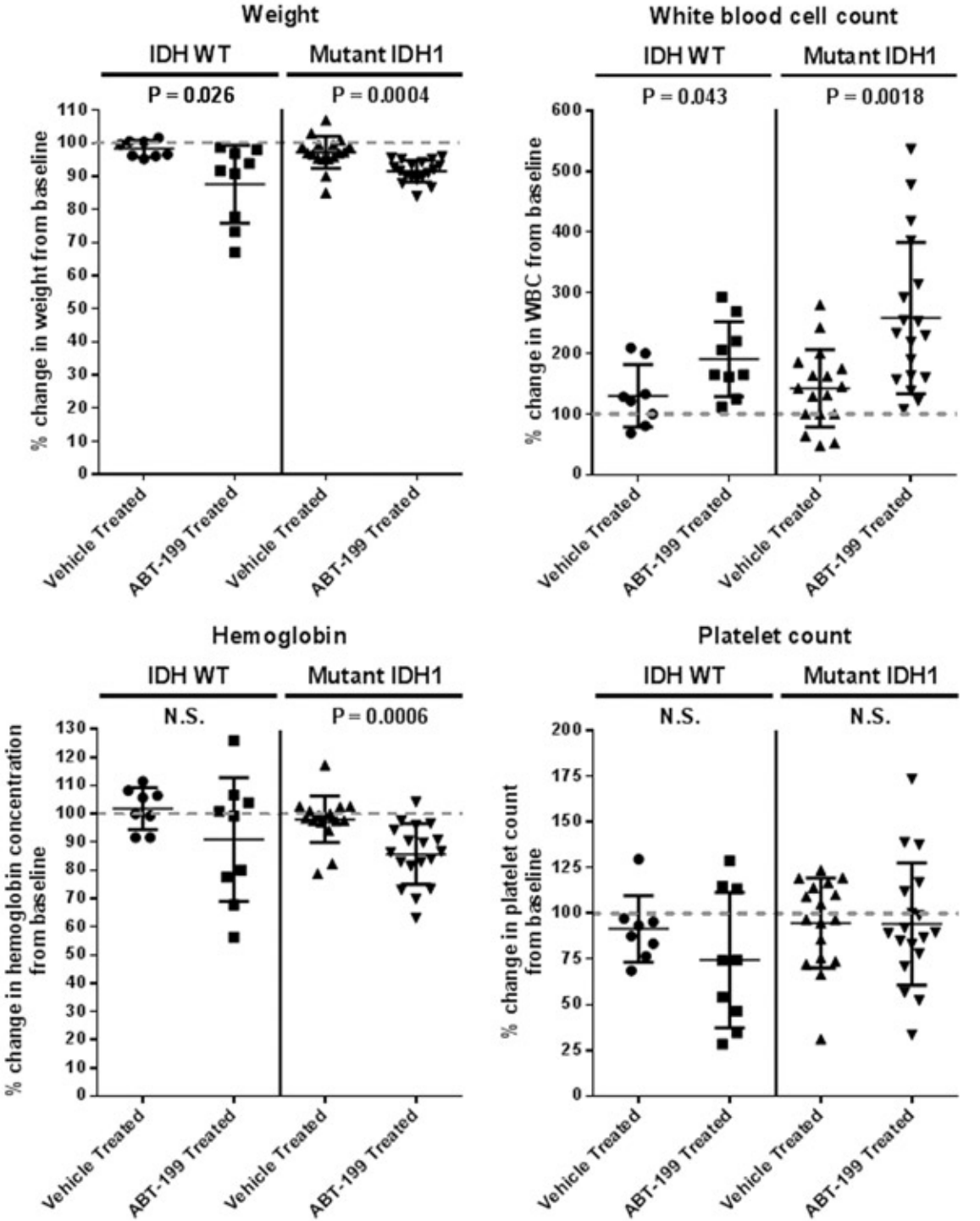

Supplementary Figure 6

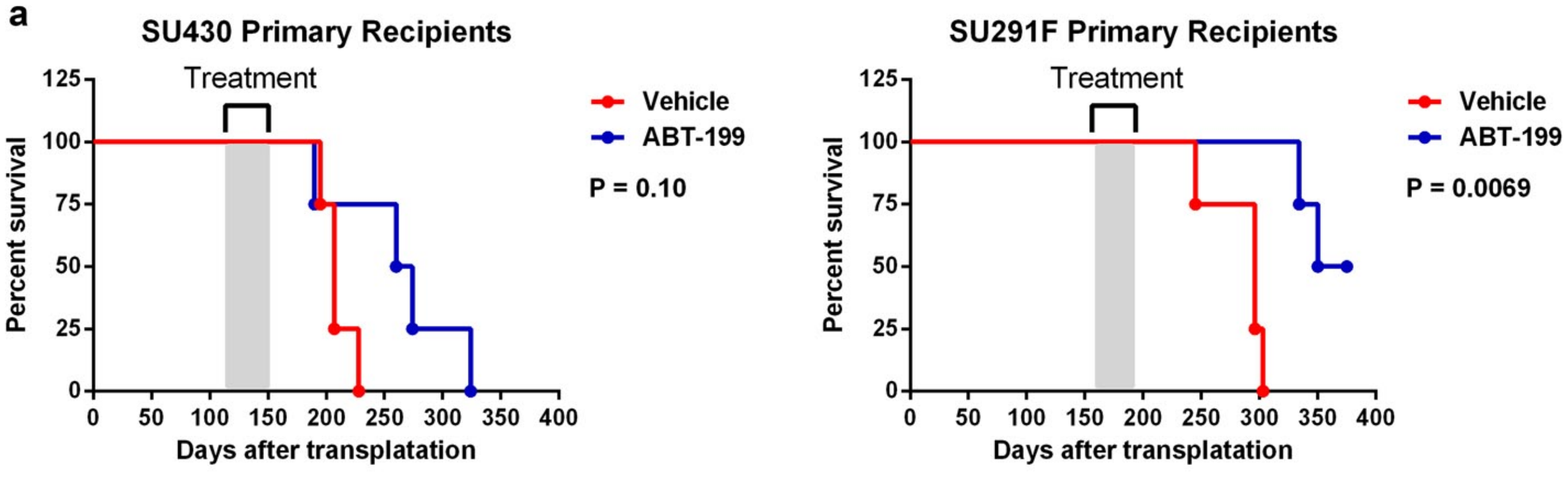

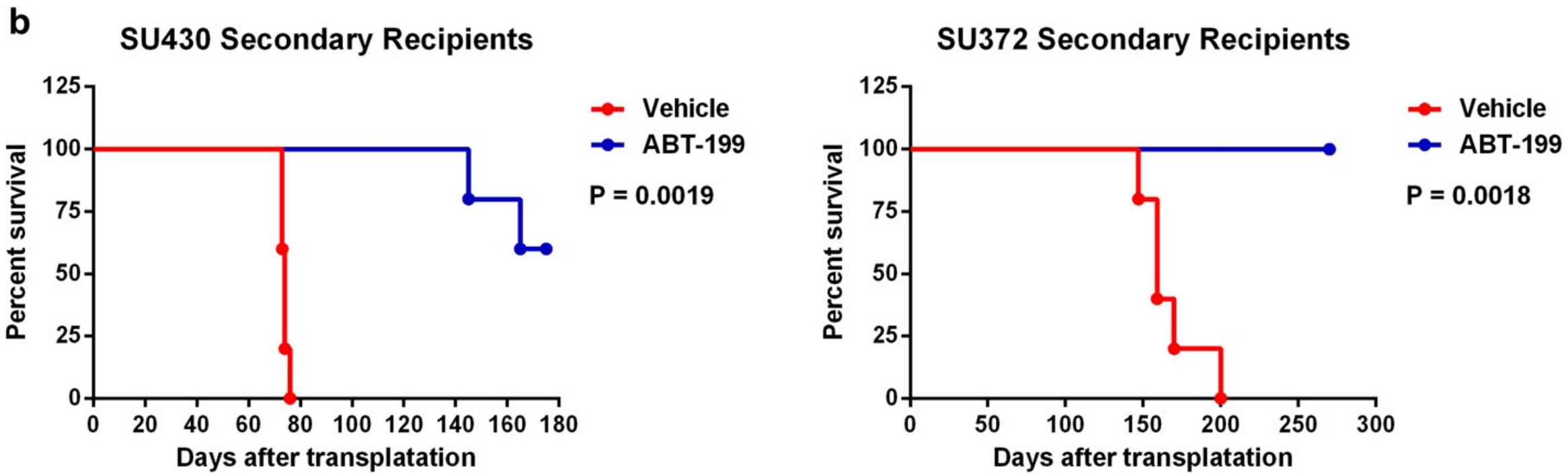

Supplementary Figure 7

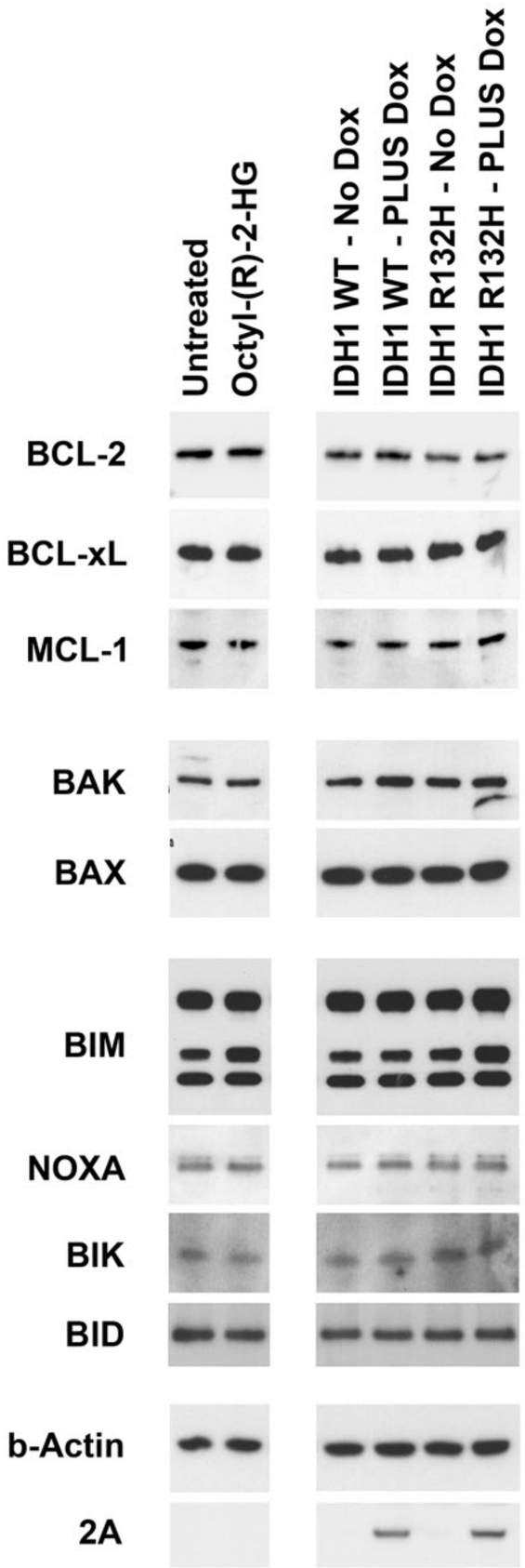

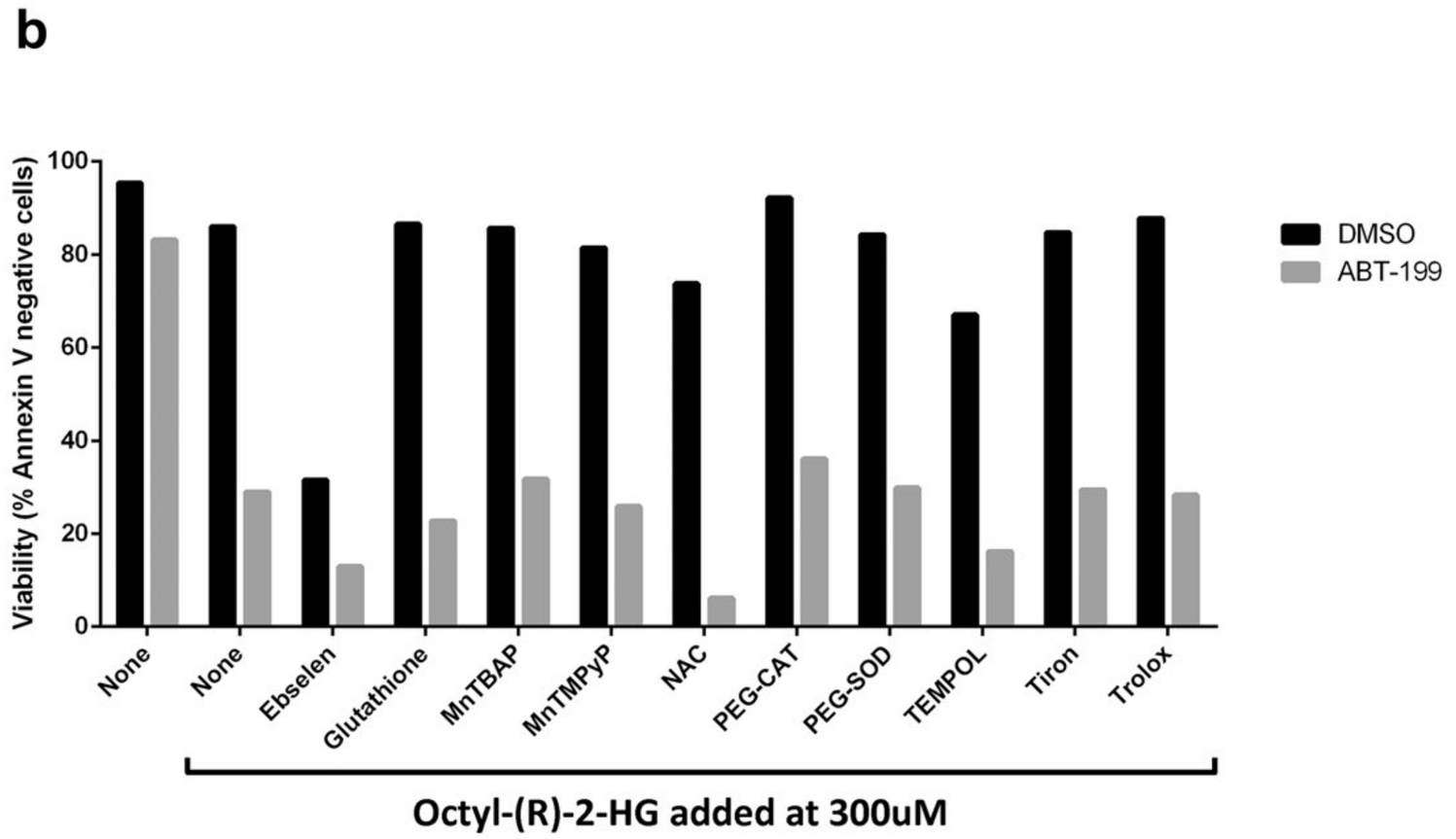

Supplementary Figure 8

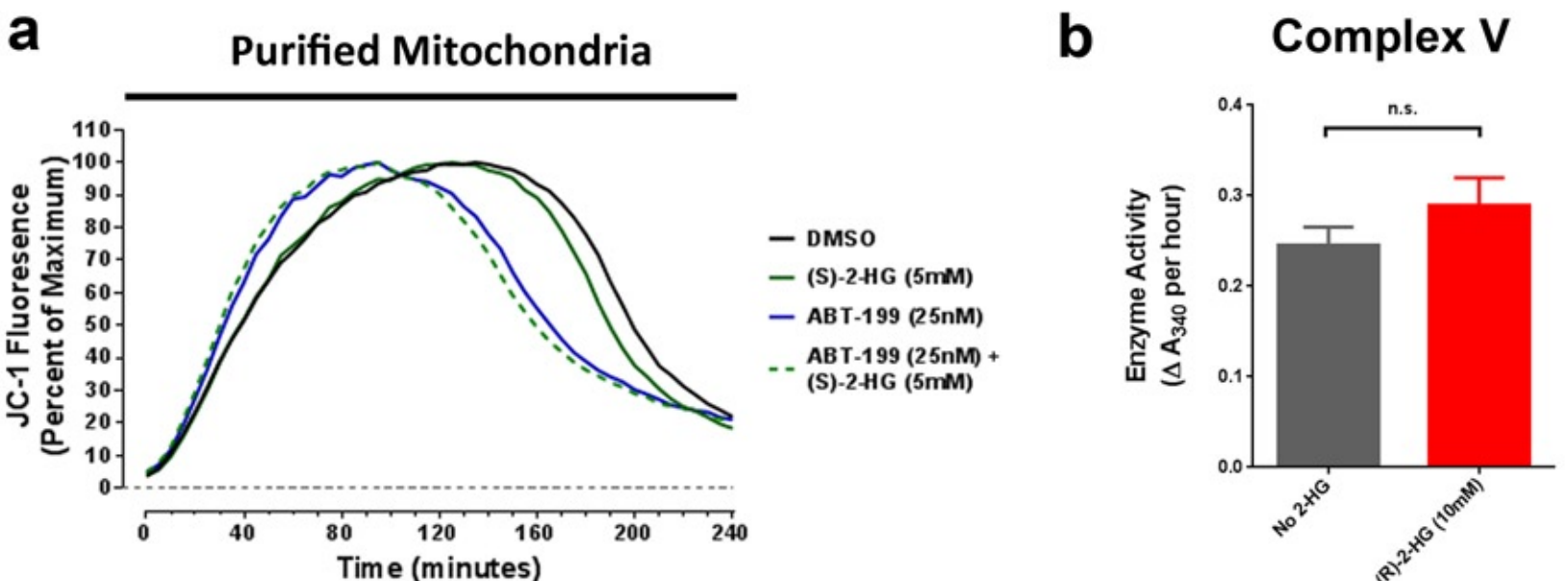

Supplementary Figure 9

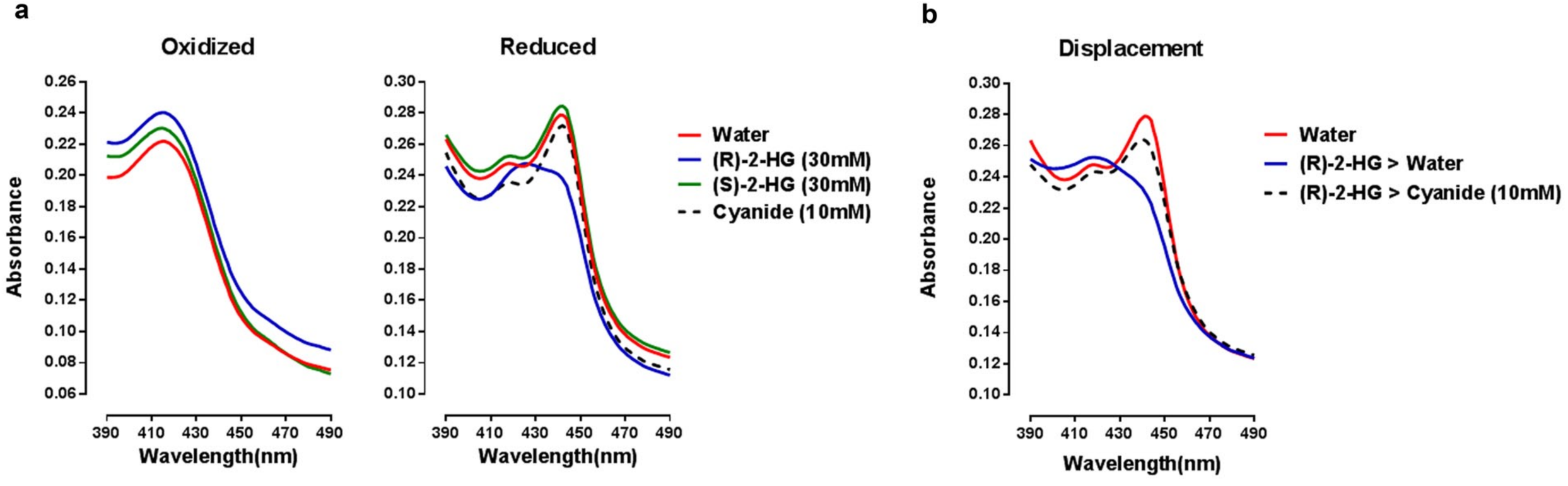

Supplementary Figure 10

a

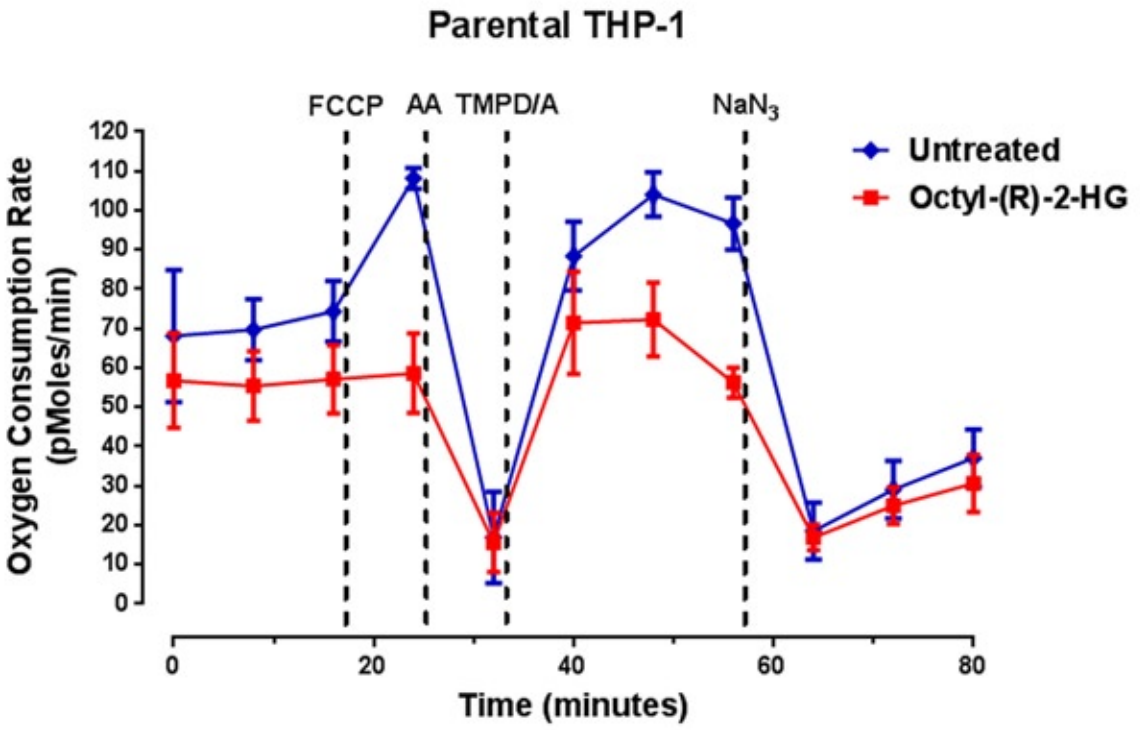

b

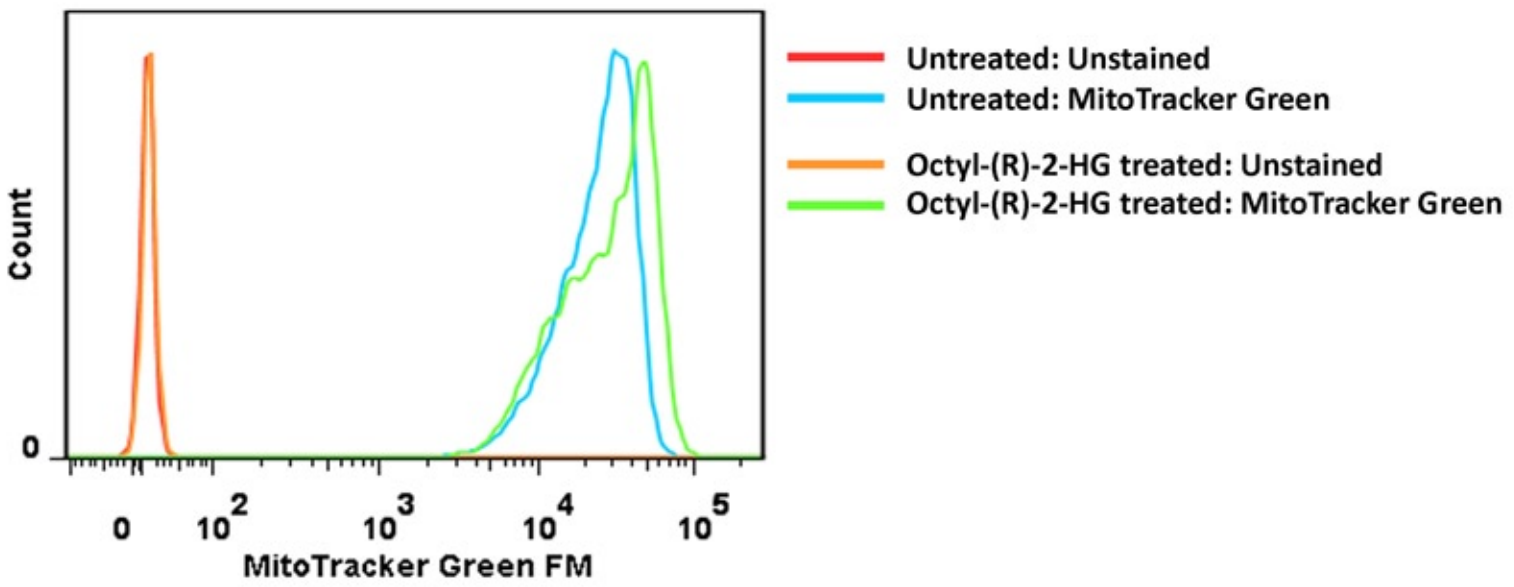

Supplementary Figure 11

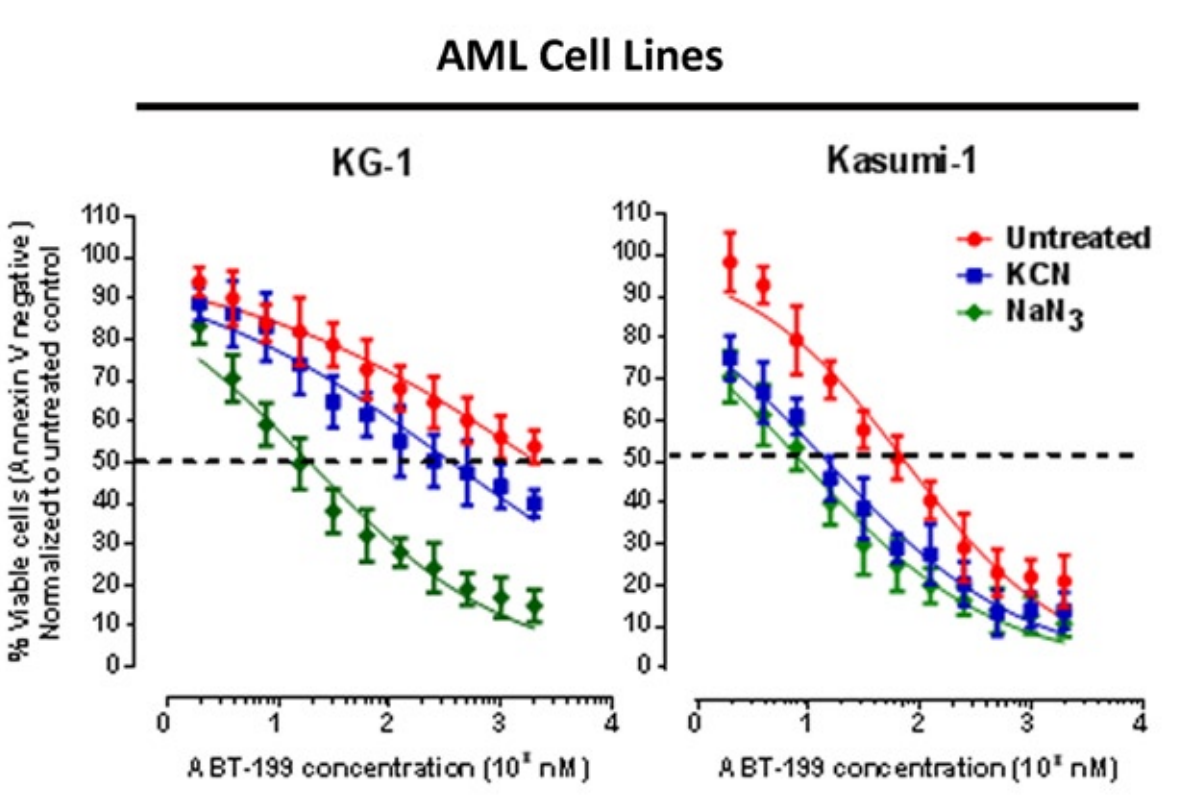

Supplementary Figure 12

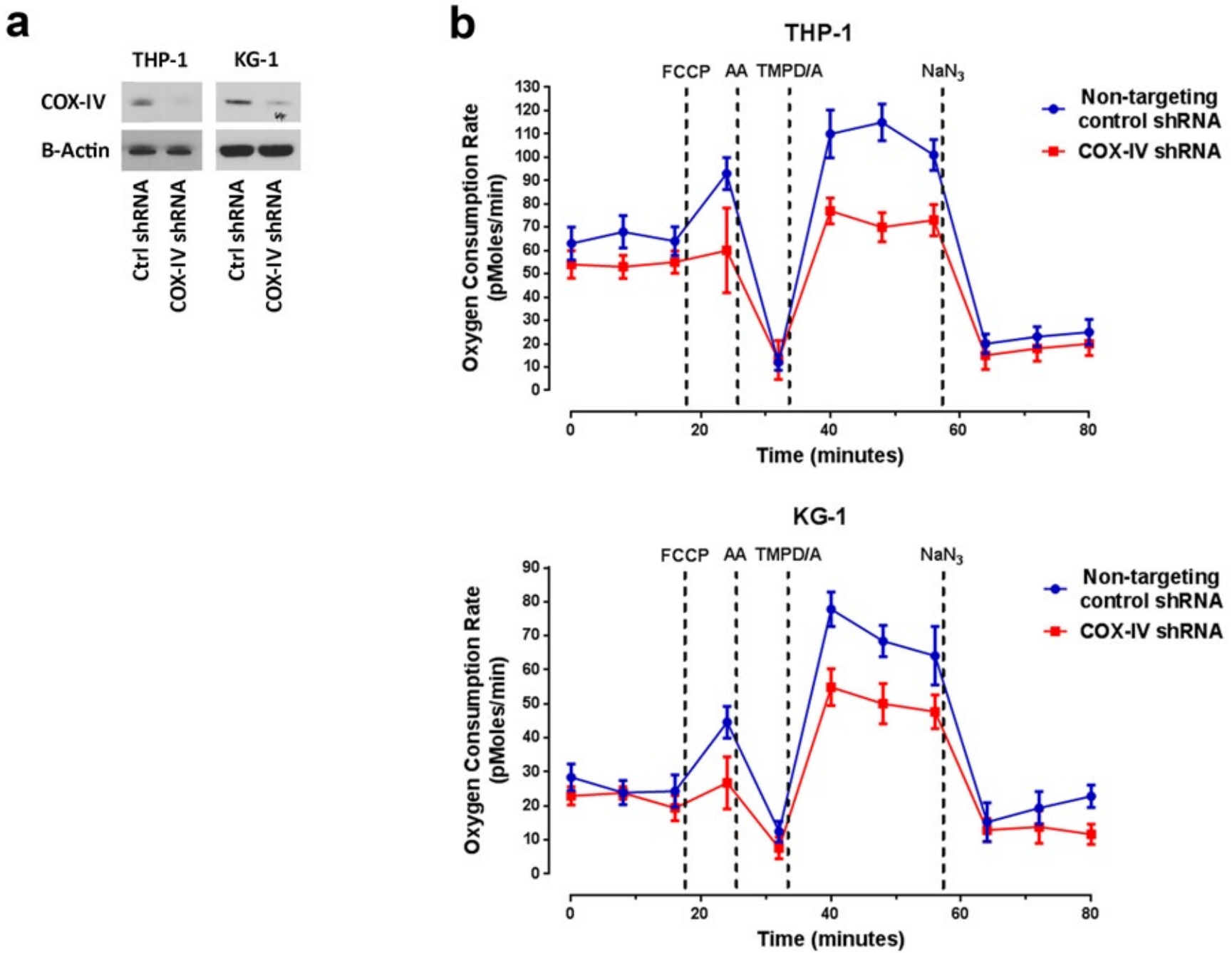

Supplementary Figure 13

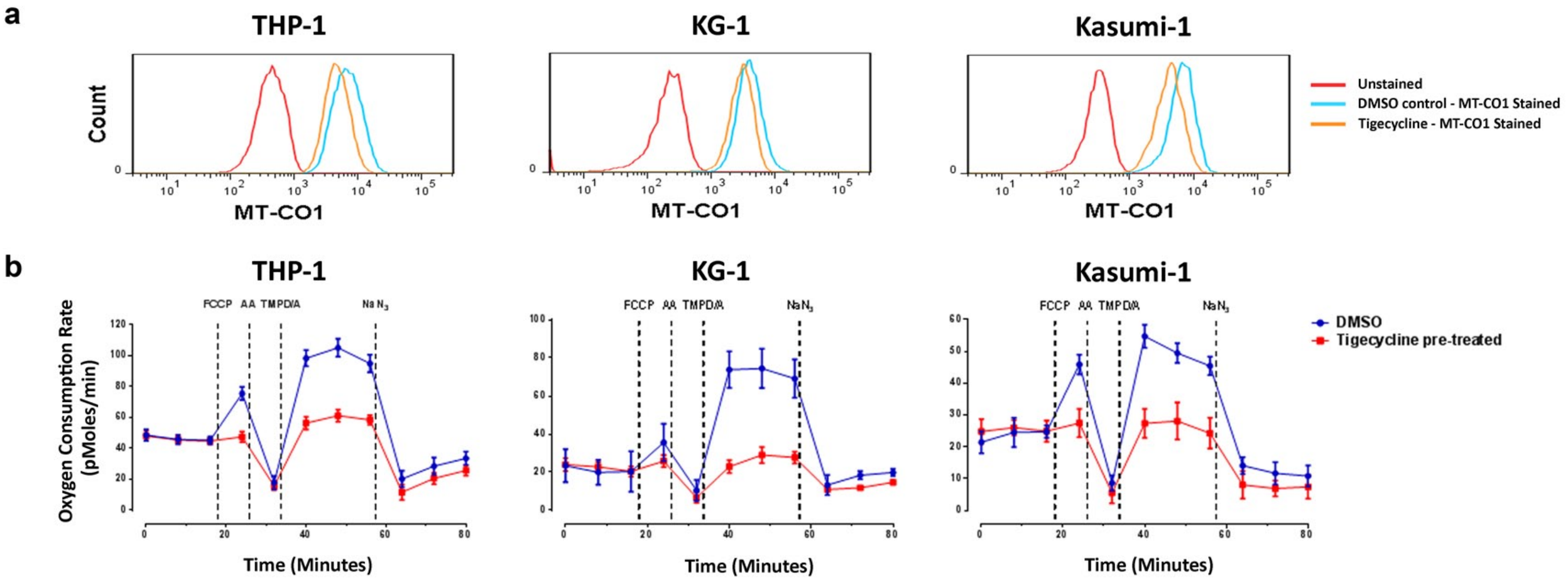

Supplementary Figure 14

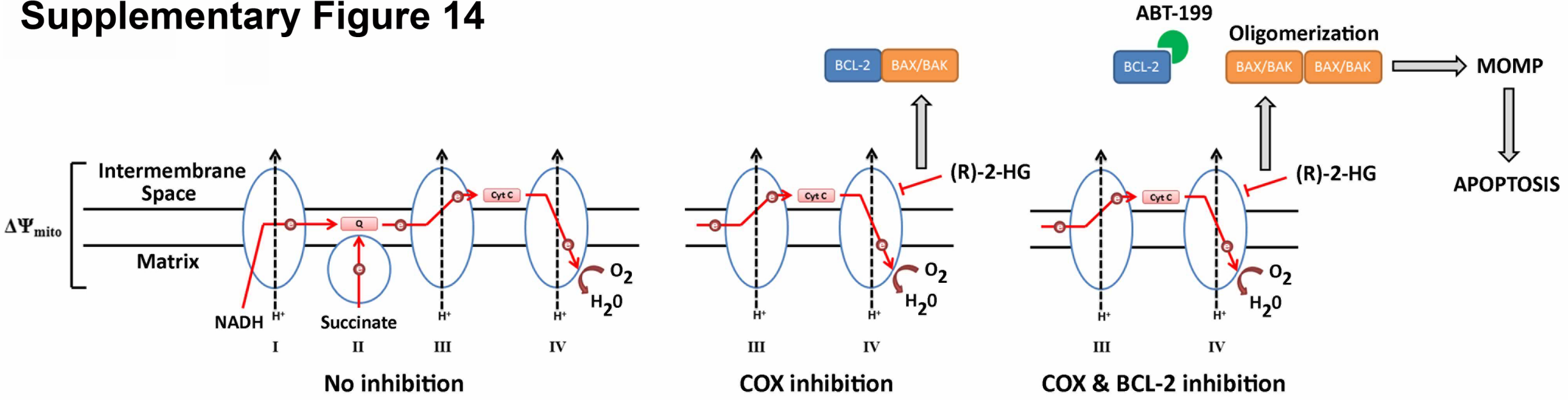

Supplementary Table 1

Rank	Gene Symbol	Gene Name	Number of redundant shRNA hits	Mean Dox/No Dox Ratio for IDH1 R132H (log_{10})	Mean Dox/No Dox Ratio for IDH1 WT (log_{10})
1	COQ5	Coenzyme Q5 Homolog, Methyltransferase	3	-0.480	0.104
2	MDC1	Mediator Of DNA-Damage Checkpoint 1	3	-0.423	-0.079
3	BCL-W (BCL2L2)	BCL2-Like 2	3	-0.414	-0.048
4	THBD	Thrombomodulin	3	-0.407	0.007
5	PLG	Plasminogen	4	-0.379	-0.092
6	CELSR1	Cadherin, EGF LAG Seven-Pass G-Type Receptor 1	3	-0.357	-0.183
7	BCL2	B-Cell CLL/Lymphoma 2	3	-0.344	-0.010
8	UBE2E1	Ubiquitin-Conjugating Enzyme E2E 1	3	-0.336	-0.082
9	SIN3A	SIN3 Transcription Regulator Family Member	4	-0.331	-0.032
10	NRIP1	Nuclear Receptor Interacting Protein 1	3	-0.320	0.115
11	LDHAL6B	Lactate Dehydrogenase A-Like 6B	3	-0.314	-0.098
12	MMS19L	MMS19 Nucleotide Excision Repair Homolog	3	-0.314	0.053
13	CACNA1B	Calcium Channel, Voltage-Dependent, N Type, Alpha 1B Subunit	3	-0.313	0.022
14	PPP2R2A	Protein Phosphatase 2, Regulatory Subunit B, Alpha	3	-0.308	-0.053
15	RAMP1	Receptor (G Protein-Coupled) Activity Modifying Protein 1	3	-0.306	0.109

Supplementary Table 2

Sample ID #	Age	Sex	Primary / Secondary	De novo / Primary refractory / Relapsed / Progression	WHO classification	Cytogenetics	IDH1/2	FLT3-ITD/TKD	NPM1c	ABT-199 IC_{50} (nM)
SU277B	70	F	Primary	Progression	AML with myelodysplasia-related changes	Normal	IDH1 R132G	Negative	Negative	3.774
SU291F	37	F	Primary	Relapsed	AML-not otherwise specified	+8	IDH1 R132H	FLT3-TKD	Positive	0.09946
SU341	28	M	Primary	De novo	AML-not otherwise specified	Normal	IDH1 R132C	Negative	Negative	0.1499
SU366B	75	M	Secondary from MDS	Collected at time of AML diagnosis	AML with myelodysplasia-related changes	Normal	IDH1 R132C	Negative	Negative	1.409
SU372	53	F	Primary	De novo	AML-not otherwise specified	Normal	IDH1 R132H	FLT3-ITD + TKD	Positive	0.648
SU419	78	M	Primary	De novo	AML-not otherwise specified	Normal	IDH1 R132C	Negative	Positive	0.8342
SU430	46	M	Primary	Primary refractory	Mixed phenotype acute leukemia (B/myeloid)	der(7)t(7;11)	IDH1 R132C	Negative	Negative	0.348
SU435B	76	M	Secondary from MDS	Collected at time of AML diagnosis	AML with myelodysplasia-related changes	+5,+8	IDH1 R132C	Negative	Negative	9.072
SU437	76	F	Secondary from CMML	Collected at time of AML diagnosis	AML with myelodysplasia-related changes	Normal	IDH1 R132H	Negative	Negative	0.0855
SU492	73	M	Primary	De novo	AML-not otherwise specified	+8	IDH1 R132C	FLT3-TKD	Negative	2.14
SU654	47	M	Primary	De novo	AML-not otherwise specified	Normal	IDH1 R132C	Negative	Positive	0.7556
SU306	32	F	Primary	De novo	AML-not otherwise specified	No analyzable metaphases	IDH2 R140Q	FLT3-TKD	Positive	4.576

SU313	50	F	Primary	De novo	AML with myelodysplasia-related changes	Normal	IDH2 R140Q	Negative	Negative	0.1172
SU339	58	M	Primary	De novo	AML with myelodysplasia-related changes	Normal	IDH2 R172K	Negative	Negative	4.217
SU351	74	M	Primary	Relapsed	AML with myelodysplasia-related changes	der(10)t(X;10),+8	IDH2 R140Q	Negative	Negative	7.977
SU424	39	M	Primary	De novo	AML with myelodysplasia-related changes	Normal	IDH2 R140Q	Negative	Positive	0.2892
SU443	68	M	Primary	De novo	AML-not otherwise specified	Normal	IDH2 R140Q	FLT3-ITD	Positive	11.63
SU450B	41	M	Primary	Relapsed	AML-not otherwise specified	Normal	IDH2 R140Q	FLT3-ITD	Positive	37.58
SU484	70	F	Primary	De novo	AML-not otherwise specified	Normal	IDH2 R140Q	Negative	Positive	0.288
SU496	24	M	Primary	Primary refractory	AML-not otherwise specified	+6,+8,+11	IDH2 R140Q	FLT3-TKD	Negative	16.08
SU572	73	M	Secondary from PV	Collected at time of AML diagnosis	AML with myelodysplasia-related changes	Unknown	IDH2 R140Q	Unknown	Unknown	0.5574
SU580	67	M	Secondary from PV	Collected at time of AML diagnosis	AML with myelodysplasia-related changes	inv(9),-19,-22	IDH2 R140Q	Negative	Negative	2.525
SU209	67	F	Primary	De novo	AML-not otherwise specified	Normal	Negative	FLT3-ITD	Positive	0.4541
SU270	60	F	Primary	Relapsed	AML-not otherwise specified	Normal	Negative	FLT3-ITD	Positive	77.82
SU325	59	F	Primary	De novo	AML-not otherwise specified	Unknown	Negative	FLT3-ITD	Positive	157
SU353	65	M	Primary	De novo	AML-not otherwise specified	Normal	Negative	FLT3-ITD	Positive	33.45

SU354	64	M	Secondary from MDS	Collected at time of AML diagnosis	AML with myelodysplasia-related changes	Trisomy 19	Negative	Negative	Negative	5.568
SU369	87	M	Primary	De novo	AML-not otherwise specified	Unknown	Negative	Negative	Negative	5.016
SU388	62	M	Primary	De novo	AML-not otherwise specified	Normal	Negative	FLT3-ITD	Negative	23.12
SU414	80	F	Primary	De novo	AML-not otherwise specified	No analyzable metaphases	Negative	Negative	Positive	50.62
SU462	86	F	Primary	De novo	AML-not otherwise specified	Unknown	Negative	FLT3-ITD	Positive	5.649
SU463	56	F	Primary	De novo	AML with myelodysplasia-related changes	57,XX,+X,+2,+10, +11,+12,+13,+14, +17,+20,+21,+22	Negative	Negative	Negative	24.75
SU524	73	M	Primary	De novo	AML-not otherwise specified	Normal	Negative	Negative	Negative	0.2813

Supplementary Table 3

Wildtype IDH Samples

Sample ID	Gender	Treatment	Baseline hCD45$^+$ CD33$^+$ CD19$^-$ Engraftment (%)	Post-Treatment hCD45$^+$ CD33$^+$ CD19$^-$ Engraftment (%)	Percent of Baseline Engraftment
SU325	Male	Mock	98.6	95	96
	Female	Mock	93.4	45.9	49
	Female	ABT-199	95	55.1	58
	Male	ABT-199	87.5	2.35	3
SU353	Female	Mock	99.2	99.7	101
	Female	Mock	67.8	81	119
	Female	Mock	98.3	83.7	85
	Female	ABT-199	99.6	9.19	9
	Female	ABT-199	98.5	97.9	99
	Female	ABT-199	99.6	84	84
SU354	Male	Mock	91	86.6	95
	Male	Mock	83.3	74.6	90
	Male	Mock	86	93.2	108
	Male	ABT-199	88.9	80.8	91
	Male	ABT-199	94.7	64.4	68
	Male	ABT-199	76.9	78.2	102
	Male	ABT-199	93	83.4	90
SU463	Female	Mock	98.9	97.9	99
	Female	Mock	99	98.4	99
	Female	Mock	98.7	99.5	101
	Female	ABT-199	99.4	95.3	96
	Female	ABT-199	99.2	98.9	100
	Female	ABT-199	99.2	98.2	99

Mutant IDH1 Samples

Sample ID	Gender	Treatment	Baseline hCD45$^+$ CD33$^+$ CD19$^-$ Engraftment (%)	Post-Treatment hCD45$^+$ CD33$^+$ CD19$^-$ Engraftment (%)	Percent of Baseline Engraftment
SU430*	Female	Mock	74.8	83.3	111
	Female	Mock	99.2	99.2	100
	Female	Mock	96	97.1	101
	Female	Mock	91.9	97.8	106
	Female	Mock	98.1	98.9	101
	Female	ABT-199	97	38.6	40
	Female	ABT-199	99.6	31.1	31

	Female	ABT-199	91.8	42.2	**46**
	Female	ABT-199	94.3	13	**14**
	Female	ABT-199	95.1	5.92	**6**
SU372	Female	Mock	45.9	33.9	**74**
	Female	Mock	11	68.5	**623**
	Female	Mock	22.2	66.9	**301**
	Female	ABT-199	36.8	13.3	**36**
	Female	ABT-199	61.7	8.67	**14**
	Female	ABT-199	21.1	9.38	**44**
SU277B	Male	Mock	21.1	19.5	**92**
	Male	ABT-199	23.1	1.4	**6**
SU437	Female	Mock	86.8	95	**109**
	Female	Mock	98.4	95.6	**97**
	Female	Mock	98.4	98.5	**100**
	Female	Mock	85.5	95.4	**112**
	Female	ABT-199	98.4	79.2	**80**
	Female	ABT-199	91.3	11.6	**13**
	Female	ABT-199	40	24.4	**61**
	Female	ABT-199	92.8	70.1	**76**
SU291F	Female	Mock	85	88	**104**
	Female	Mock	71	85	**120**
	Female	Mock	96	95	**99**
	Female	Mock	94	85	**90**
	Female	ABT-199	**77**	**22**	**29**
	Female	ABT-199	**78**	**12**	**15**
	Female	ABT-199	**97**	**8**	**8**
	Female	ABT-199	**61**	**45**	**74**
	Female	ABT-199	**97**	**22**	**23**

* SU430 is a mixed phenotype acute leukemia sample (B/myeloid) with variable CD33 and CD19 expression on blasts. Leukemic engraftment of SU430 was determined based on human CD45 expression alone.

Supplementary Table 4

Sample	Genotype	MT-CO1 expression	COX activity	Normalized COX activity
SU277B	IDH1	22.69	50	2.22
SU291F	IDH1	24.77	168	6.77
SU366	IDH1	17.83	119	6.66
SU430	IDH1	13.92	51	3.63
SU654	IDH1	32.65	114	3.48
SU306	IDH2	26.93	153	5.68
SU484	IDH2	19.12	22	1.13
SU270	WT	8.91	107	11.99
SU325	WT	19.53	145	7.42
SU353	WT	18.71	175	9.36
SU388	WT	17.40	80	4.59
SU463	WT	5.93	50	8.36
SU595	WT	9.39	109	11.61
SU623	WT	17.67	131	7.41